Journal of Applied Electrochemistry **00**: 1–6, 2004.

Electroreduction-oxidation and quantitative determination of CO_2 on a new SPE-based system

JUN LIU, HEQING YAN*, KANGLI WANG and E'FENG WANG
College of chemistry and molecular science, Wuhan University, Wuhan 430072, People's Republic of China
*(*author for correspondence: fax: +86-27-8764-7617, e-mail: h.q.yan@263.net)*

Received ■; accepted in revised form ■

Key words: anodic stripping voltammetry, CO_2, electroreduction, solid polymer electrolyte (SPE), sensor

Abstract

Electroreduction–oxidation of CO_2 was studied by anodic stripping voltammetry on different SPE electrodes. The catalytic capacity of these electrodes for CO_2 electroreduction was examined by comparing the oxidation charges of both the products ($R(CO_2)$) produced by electroreduction of CO_2 (Q_{ox}) and the adsorbed hydrogen (Q_H). SEM analysis was used to understand the catalytic capacity of different electrodes. A new electrochemical system based on a PtAu-SPE electrode, which had the best comprehensive catalytic capacity among the investigated electrodes, showed a satisfactory linear response (Q_{ox}) to CO_2 concentration in the range 0–40% when adsorption time $t_{ad} \leqslant 1$ min. In addition, this system possessed advantages such as no leakage, high efficiency, excellent reproducibility and good stability. Furthermore, the composition of $R(CO_2)$ on the Pt-SPE and the Pt alloy-SPE electrodes was investigated by XPS analysis.

1. Introduction

Quantitative determination of CO_2 is very important in environmental protection, medical diagnosis and industrial safety control. However, it is difficult to detect CO_2 directly by chemical methods due to the stability of the molecule.

The Stow–Severinghaus sensor [1] detects CO_2 indirectly by measuring the pH-shift of a bicarbonate electrolyte, its application is limited by the logarithmic response behavior and the interference by other pH-shifting gases.

Giner observed that CO_2 can be reduced by adsorbed hydrogen atoms (H_{ad}), forming 'reduced' CO_2 ($R(CO_2)$) on a Pt working electrode when the electrode was kept at the potential of hydrogen adsorption in an acidic solution. This process could be expressed by the equation: $CO_2 + Had \rightarrow R(CO_2)$. $R(CO_2)$ could be oxidized quantitatively when an anodic scanning potential was applied to the working electrode. Thus CO_2 could be indirectly determined [2, 3]. This electrochemical technique for CO_2 detection was called anodic stripping voltammetry (ASV). Subsequently, electroreduction-oxidation and/or quantitative determination of CO_2 on noble metal electrodes in the acidic solution has been much studied [4–8]. These CO_2 detection systems using ASV suffered from leakage problems and a relatively low efficiency because liquid electrolyte has to be used. Solid polymer electrolyte (SPE) provides the possibility to design a solid-state electrochemical system [9] without leakage, and the chemical plating method described by Takenaka and Torikai (abbreviated as 'T–T method') [10] makes it feasible to fabricate a highly efficient electrode on a Nafion membrane (a kind of SPE) for the reduction or oxidation of a gas directly in the vapor phase. Based on the concepts above, a new type of SPE-hydrophobic gas diffusion electrode [11] was designed and subsequently SPE-O_2 [12, 13], SPE-CO [14] and SPE-H_2S [15, 16] sensors were successfully developed.

In this study, different SPE electrodes were prepared for the construction of a CO_2 detection system. The catalytic capacity of these electrodes for CO_2 electroreduction was investigated by both ASV and SEM. The electrode with the best comprehensive catalytic capacity (i.e. the PtAu-SPE electrode) was chosen to further fabricate a highly efficient CO_2 detection system. In addition, the composition of CO_2 electroreduction products ($R(CO_2)$) on the Pt-SPE and the Pt alloy-SPE electrodes were examined by XPS. Data for the output signals of the system were repeated at least three times and the reproducibility of the data is within ±0.5%. To the best of our knowledge, this study is the first to report the use of the PtAu-SPE electrode based system to quantitatively determine CO_2 concentration.

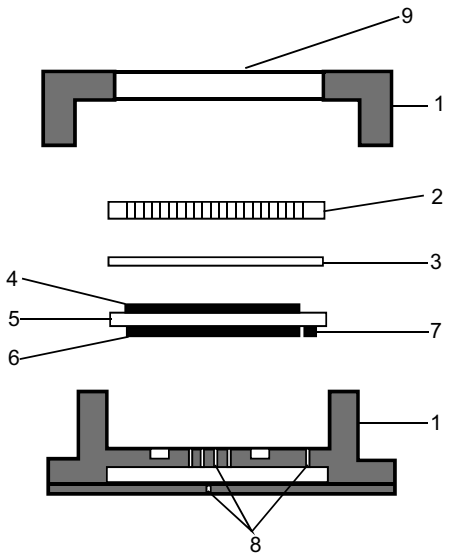

Fig. 1. Scheme of the SPE-based system for CO_2 detection. (1) Plastic shell; (2) perforated Teflon plate; (3) Teflon membrane; (4) working electrode; (5) Nafion membrane; (6) counter electrode; (7) reference electrode; (8) opening to air; (9) sample gas inlet.

2. Experimental

The SPE-based system is shown schematically in Figure 1. Acid-treated ($HClO_4$, 4 mol l^{-1}) Nafion® 117 membrane (perfluorinated sulfonic cation-exchange membrane, Du Pont) was used as SPE membrane.

2.1. *Preparation of the working electrode*

The working electrode (named SPE electrode in this paper, $S = 0.5$ cm^2) was prepared according to the T-T method [10] with a two-compartment glass tube. The noble metal salt solution was in one compartment and the reducing agent ($NaBH_4$ or N_2H_4 solution) was in the other, and these two compartments were separated by a piece of Nafion film. The Pt-SPE or the Au-SPE electrode was prepared by reducing 2.5 ml H_2PtCl_6 or $HAuCl_4$ into Pt or Au on the Nafion film. The PtRh-SPE electrode was prepared by reducing noble metal salt mixtures (2 ml H_2PtCl_6 and 0.5 ml H_3RhCl_6). The PtAu-SPE electrode was prepared by first depositing a Au layer on the Nafion film from 0.5 ml $HAuCl_4$, followed by a Pt layer from 2 ml H_2PtCl_6. The RhAu-SPE electrode was prepared using the same procedure as that of the PtAu-SPE electrode preparation, the only difference being that the deposition layer was Rh from 2 ml H_3RhCl_6. All concentrations of the noble metal salts were 0.02 mol l^{-1}.

2.2. *Preparation of counter and reference electrodes*

Two pieces of Teflon-bonded Pt black membrane were mechanically pressed onto one side of the Nafion membrane; the larger one ($S = 0.5$ cm^2) served as counter electrode, and the smaller one ($S = 0.1$ cm^2), which faced the surrounding air, served as reference electrode.

Finally, these SPE electrodes were dipped in 4 mol l^{-1} H_2SO_4 for 24 h before they were set in the detection system as shown in Figure 1.

2.3. *Instrumental measurements*

Electrochemical measurements were conducted with a SHD-1 pontentiostat (Yanbian Electrochemical Instruments Factory, China) and a 4086 X-Y recorder (The Fourth Instruments Factory of Chongqing, China). All gases were provided by Beifen Company of Beijing (CO_2 of different concentrations were prepared by diluting CO_2 with N_2).

SEM analysis was conducted with a X-650 scanning electron microanalyser (HITACHI). XPS analysis was conducted with a XSAM800 instrument (KRATOS). The Mg-K_α target at 1253.6 eV and 16 mA × 12.5 kV was used in the experiment. The samples were detected under 2×10^{-7} Pa and the reference energy was vs C_{1s} (284.6 eV).

All experiments were carried out at room temperature. All potentials were measured vs a Pt/air reference electrode and all gas flow rates were 40 ml min^{-1}.

3. Results and discussion

3.1. *Catalyst selection for CO_2 electroreduction*

The main aim of the experiments of this part was to compare the catalytic capacity of different SPE electrodes for CO_2 electroreduction and to select the best for the fabrication of a CO_2 detection system.

The electroreduction–oxidation of CO_2 on different SPE electrodes was studied by ASV. Before the measurement, the working electrode was scanned repeatedly under pure N_2 ($\geqslant$99.999%) between −1.15 and 0.5 V

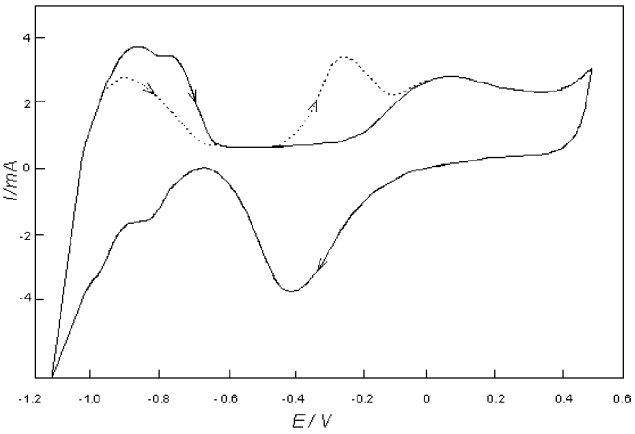

Fig. 2. The typical voltammogram on Pt-SPE electrode. Solid curve, cyclic voltammogram in pure N_2 atomosphere; dotted curve; anodic stripping voltammogram after adsorbing CO_2 for 5 min (E_{ad} (CO_2 adsorption potential) = −0.95 V; Scan rate = 20 mV s^{-1}; Scan direction: as the arrowhead shown).

until a reproducible cyclic voltammogram appeared. The working electrode was then kept in the potential range of hydrogen adsorption and the gas supply was switched to pure CO_2 ($\geqslant$99.995%) for 5 min. CO_2 was then removed with a N_2 stream and an anodic scanning voltammogram was recorded. A typical voltammogram is shown in Figure 2.

An oxidation peak of $R(CO_2)$ was observed on a Pt-SPE electrode. Similar phenomena were observed on the PtAu-SPE, the PtRh-SPE and the RhAu-SPE electrodes with the exception of the Au-SPE electrodes. This indicates that only a SPE electrode containing Pt or Rh has catalytic capacity for CO_2 electroreduction. This result is in agreement with the study of Vassiliev et al. [4].

The oxidation charge of $R(CO_2)$ (Q_{ox}), which can be calculated by integrating the oxidation current peak of $R(CO_2)$, is an important parameter to evaluate the catalytic capacity to CO_2 electroreduction. The relationships between Q_{ox} and E_{ad} on different SPE electrodes are shown in Figure 3. Curves 2 and 3 in Figure 3, corresponding to electrodes not containing Rh, have the same shape and their E_{ad} for the maximal Q_{ox} are −1.0 V. However, curves 1 and 4, corresponding to the Rh-containing electrodes, have different shapes, and their E_{ad} for the maximal Q_{ox} shift negatively. This negative shift of the E_{ad} for the maximal Q_{ox} of the Rh-containing electrode may be explained on the basis of the greater adsorbability of the sulphate ion on Rh as compared to Pt [6]. This implies that the process and products of CO_2 electroreduction on Rh-containing electrodes may be different from those on electrodes not containing Rh. It is also shown in Figure 3 that CO_2 can be reduced in the hydrogen evolution region on these SPE electrodes. This is in accord with the study of Taguchi et al. for noble metal electrodes in solution [17]. The RhAu-SPE electrode was not investigated in the

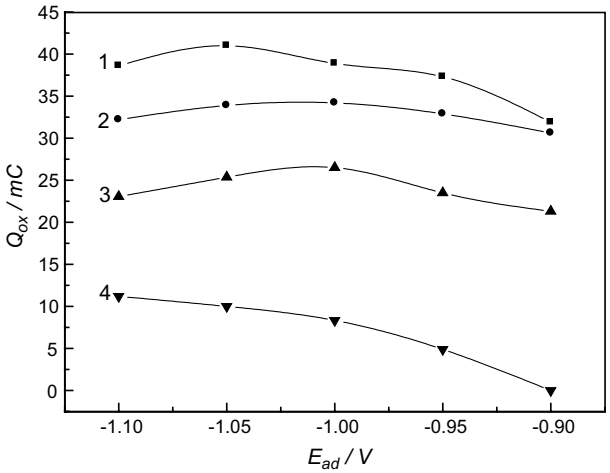

Fig. 3. The relationship between Q_{ox} and E_{ad} on different SPE electrodes. (■), the PtRh-SPE electrode; (●), the PtAu-SPE electrode; (▲), the Pt-SPE electrode; (▼), the RhAu-SPE electrode.

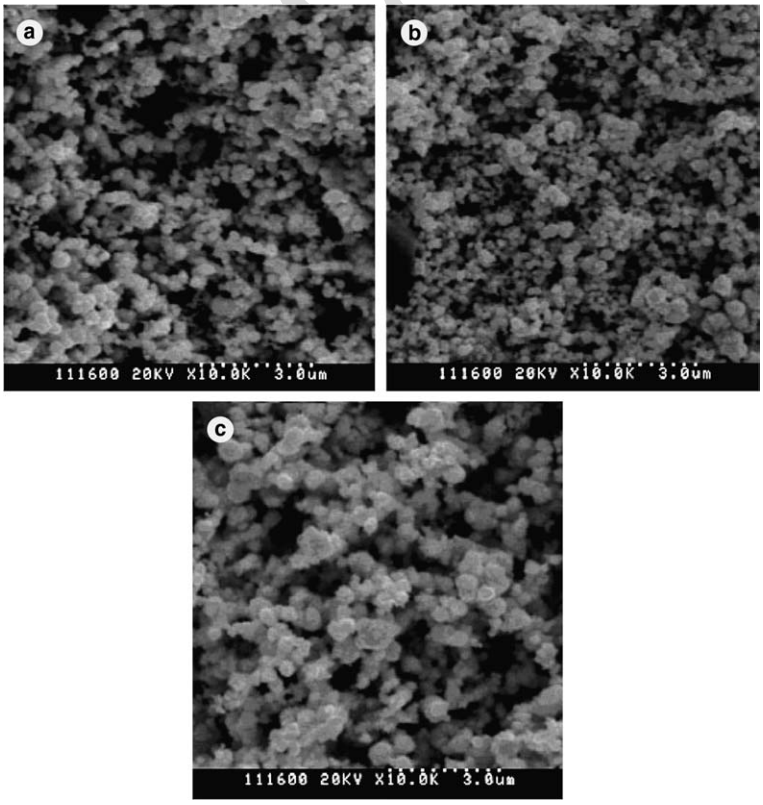

Fig. 4. SEM top views of the Pt-SPE and the Pt alloy-SPE electrodes. (a) the PtRh-SPE electrode; (b) the PtAu-SPE electrode; (c) the Pt-SPE electrode.

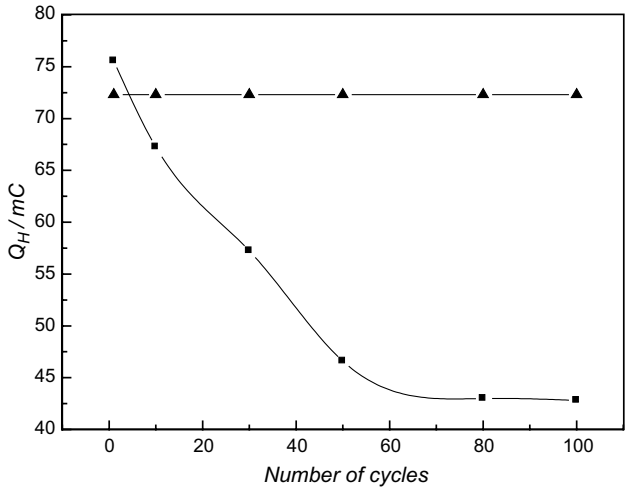

Fig. 5. The decay curves of Q_H in N_2. (■), the PtRh-SPE electrode; (▲), the PtAu-SPE electrode.

following study because its catalytic capacity is much poorer than that of the other electrodes.

Furthermore, Figure 3 indicates that the catalytic capacity of the Pt alloy-SPE electrode is higher than that of the Pt-SPE electrode. The fact is probably attributable to the larger specific surface of the Pt alloy-SPE electrodes. The area of the specific surface can be reflected by the roughness factor (RF) which is the ratio of the real-to-geometric surface area. The RF values of the electrodes corresponding to curve 1, 2 and 3 in Figure 3 are 726, 705 and 487 respectively. This indicates that the specific surface of the Pt alloy-SPE electrode is much larger than that of the Pt-SPE electrode. The SEM top views of the Pt-SPE and the Pt alloy-SPE electrodes are shown in Figure 4. It is obvious that the average diameter of the particles of the Pt alloy-SPE electrode is much smaller than that of the Pt-SPE electrode. Therefore, SEM analysis strongly supported the conclusion. It should be mentioned that the catalytic capacity of an electrode is governed by two factors, one is the nature of the catalyst, the other is the specific surface area of the catalyst. For the PtRh-SPE electrode, besides having high specific area, the nature of both Pt and Rh having catalytic capacity for CO_2 electroreduction is another reason leading to the excellent catalytic capacity of the PtRh-SPE electrode.

The oxidation charge of H_{ad} (Q_H), which can be calculated by integrating the oxidation current peak of H_{ad} in the voltammogram, reflects the amount of H_{ad}. According to the equation: $CO_2 + \mathrm{Had} \rightarrow \mathrm{R}(CO_2)$, the catalytic capacity of an electrode depends on the amount of H_{ad}. Thus Q_H is another important parameter in evaluating the catalytic capacity of the electrode to CO_2 electroreduction. The Q_H decay curves of the PtRh-SPE and the PtAu-SPE electrodes are shown in Figure 5 for comparison. The first cycle of the decay curves was determined by the appearance of the first reproducible cyclic voltammogram of a SPE electrode. Q_H of the PtRh-SPE electrode decreased sharply with increasing cycle number. This means that the decay of the catalytic capacity of the PtRh-SPE electrode is serious. This is probably due to the dissolution of Rh at the interface of the alloy layer and the Nafion film, which can cause both the loss of Rh and disconnection of metal particles of the alloy layer. In contrast, the PtAu-SPE electrode showed no decrease in Q_H with increased scanning. This indicates that the PtAu-SPE electrode is much more stable than the PtRh-SPE electrode in acid conditions and the catalytic capacity of the former electrode is higher than that of the latter in the long run. Therefore, the PtAu-SPE electrode had the best catalytic capacity among the investigated electrodes and it was selected for the fabrication of a CO_2 detection system.

3.2. *Quantitative determination of CO_2 on the PtAu-SPE based system*

In the PtAu-SPE based system, the PtAu-SPE electrode worked as the sensing electrode and a piece of gas diffusion-limiting membrane (Teflon membrane) was placed on it to maintain the CO_2 flux constant. E_{ad} was controlled at −1.00 V for CO_2 adsorption. According to Giner [18], when keeping t_{ad} at a relatively low value with other parameters, being maintained constant, CO_2 electroreduction is controlled by CO_2 diffusion, and Q_{ox} is proportional to CO_2 concentration. A plot of Q_{ox} against CO_2 concentration at different t_{ad} is shown in Figure 6. In the concentration range 0–40%, Q_{ox} increases linearly with CO_2 concentration when $t_{ad} \leqslant 1$ min, but when $t_{ad} > 1$ min, the relationship between Q_{ox} and CO_2 concentration is not linear. This result is consistent with that reported for a Pt electrode in acidic solution [5]. It is also shown in Figure 6 that even when $t_{ad} > 1$min, Q_{ox} is proportional to CO_2 concentration in a relatively narrow concentration range

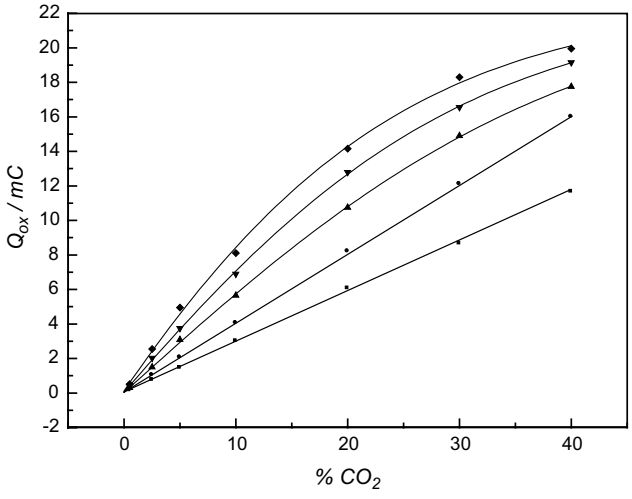

Fig. 6. A plot of Q_{ox} against CO_2 concentration at different t_{ad}. (■), $t_{ad} = 30$ s; (●), $t_{ad} = 1$ min; (▲), $t_{ad} = 2$ min; (▼), $t_{ad} = 3$ min; (♦), $t_{ad} = 4$ min.

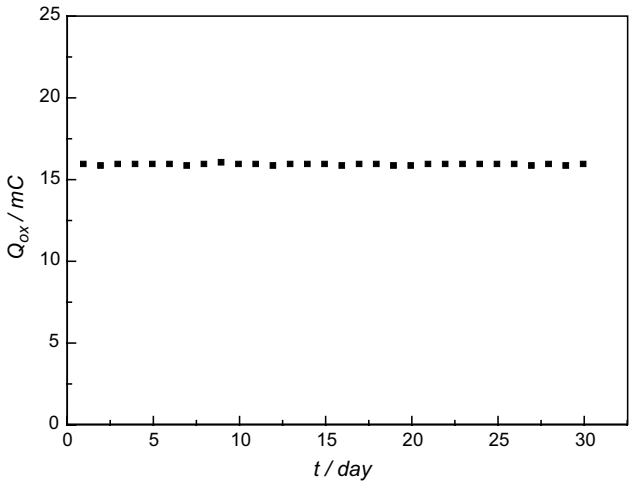

Fig. 7. The relationship of the output signals (Q_{ox}) with time on the PtAu-SPE electrode based system.

of CO_2. These facts imply that either high CO_2 concentration or long t_{ad} causes high coverage of $R(CO_2)$ on the working electrode. This makes the electrode process of CO_2 electroreduction no longer CO_2 diffusion controlled and the deviation of the relationship of Q_{ox} and CO_2 concentration from linearity is observed.

3.3. *Stability of the output signals (Q_{ox})*

Stability of the output signals (Q_{ox}) of the PtAu-SPE electrode based system was consecutively tested for one month (30 days). The potential of the working electrode was kept at −1.00 V for CO_2 adsorption. Forty percent CO_2 (flow rate = 40 ml min^{-1}) was introduced into the system for 1 min per day. The relationship of the output signals (Q_{ox}) with time is shown in Figure 7. The output signal shows almost no change in one month, indicating that the PtAu-SPE electrode based system possesses the advantage of good stability.

3.4. *XPS analysis of $R(CO_2)$*

The analysis of $R(CO_2)$ compositions on the Pt-SPE and the Pt alloy-SPE electrodes was carried out by XPS peak-fitted-analysis. As shown in Figure 8, the fitted curve (the dashed line), accumulated by the characteristic curves of C-containing compound (the dotted line), agreed very well with the original curve (the solid line) in the energy range 282.0–292.0 eV (the binding energy scope of the C-containing compounds). This means, in this energy range the original curve can be regarded as the accumulation of the dotted lines. Therefore, information about the $R(CO_2)$ adsorbates on the SPE

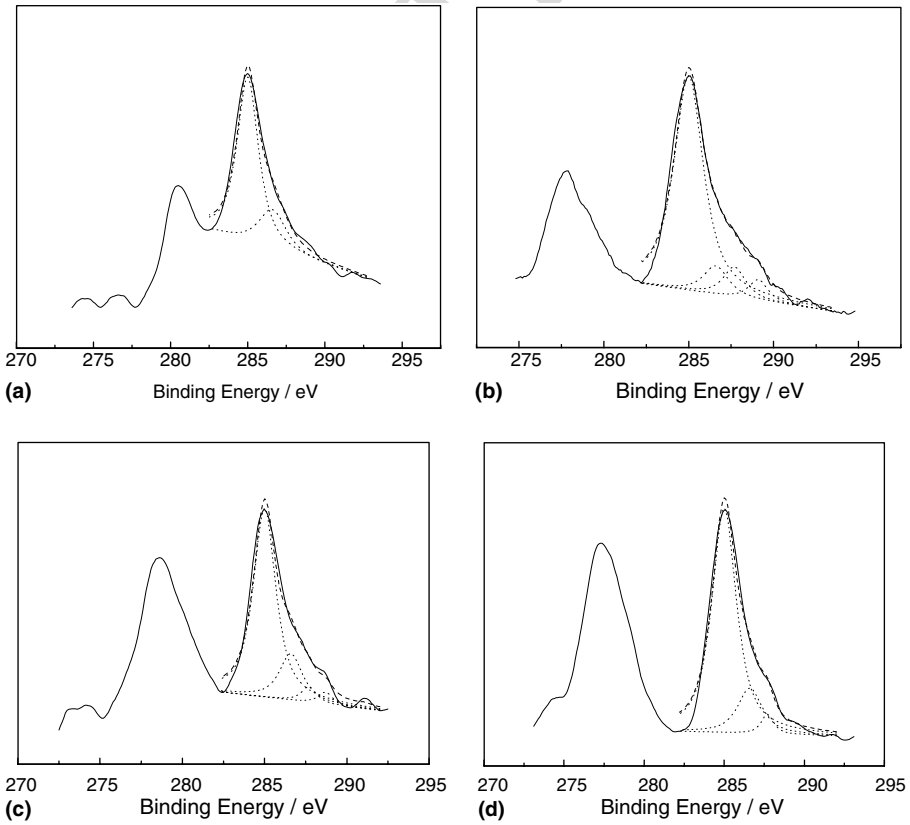

Fig. 8. XPS peak-fitted-analysis of $R(CO_2)$ on Pt-SPE and Pt alloy-SPE electrodes. (a) Blank SPE film; (b) Pt-SPE electrode; (c) PtAu-SPE electrode; (d) PtRh-SPE electrode; $R(CO_2)$ are all formed at E_{ad} = −1.00 V. ——, the original curve recorded by XPS apparatus, includes information of all C-containing compounds adsorbed on the SPE electrode; ·····, the characteristic curve of different C-containing compound; - - - - -, the fitted curve for simulation of the original one, accumulated by dotted curves. (The peaks of the original curve, whose bonding energy is under 282.0 eV, are induced by impurities of the XPS system.)

electrode, which were recorded by the original curve, could be actually reflected by the dotted lines. Compared with Figure 8 (a) (the background graph), there are two more dotted lines in both Figure 8(b) and (c). According to the peak binding energy at 287.7 eV and ca. 289.0 eV, these two dotted lines represent the characteristic curves of –CO– and $–COO^-$ respectively. Similarly, the further dotted line in Figure 8(d) represents the characteristic curves of –CO–. That is to say, the components of $R(CO_2)$ on the Pt-SPE and the PtAu-SPE electrodes are the same, but differ from that on the PtRh-SPE electrode. This corroborates the conjecture that the process and products of CO_2 electroreduction on Rh-containing electrodes may be different from those on the other electrodes in Section 3.1.

4. Conclusion

The catalytic capacity of different SPE electrodes for CO_2 electroreduction was investigated by both ASV and SEM. The initial catalytic capacity of the PtRh-SPE electrode was very high, but this electrode was very unstable under cyclic scanning, this being probably due to Rh dissolution. The PtAu-SPE electrode was found to have an excellent comprehensive catalytic capacity and was selected as the sensing electrode for the CO_2 detection system. This system showed a satisfactory linear response (Q_{ox}) to CO_2 concentration (0–40%) when $t_{ad} \leqslant 1$ min. In addition, this system has a number of other attractive advantages, such as high efficiency, no leakage problem, high catalytic capacity, excellent reproducibility and good stability. Hence, this PtAu-SPE based system shows promise for development as a practical CO_2 sensor.

XPS analysis showed that $R(CO_2)$ adsorbed on the Pt-SPE or the PtAu-SPE electrode included –CO– and $–COO^-$, while that adsorbed on the PtRh-SPE electrode only included –CO–, thus suggesting a different mechanism of CO_2 electroreduction on the PtRh-SPE electrode.

Acknowledgement

The authors thank the National Natural Science Foundation of China for financial support (Grant no.107880233).

References

1. J.W. Severinghaus and A.F. Bradley, *J. Appl. Physiol.* **13** (1958) 515.
2. J. Giner, *Electrochim. Acta* **8** (1963) 857.
3. J. Giner, *Electrochim. Acta* **9** (1964) 63.
4. Yu.B. Vassiliev, V.S. Bagotzky, N.V. Osetrova and A. Mikhailova, *J. Electroanal. Chem.* **189** (1985) 311.
5. A. kuver and W. Vielstich, *J. Electroanal. Chem.* **353** (1993) 255.
6. M.L. Marcos, J. Gonzalez-Velasco, A.E. Bolzan and A.J. Arvia, *J. Electroanal. Chem.* **395** (1995) 91.
7. N. Hoshi, M. Noma, T. Suzuki and Y. Hori, *J. Electroanal. Chem.* **421** (1997) 15.
8. M. Grden, A. Paruszewska and A. Czerwinski, *J. Electroanal. Chem.* **502** (2001) 91.
9. F. Opekar, *J. Electroanal. Chem.* **260** (1989) 451.
10. H. Takenaka and E. Torikai, *Kokai Tokkyo Koho* (*Japan Patent*) **55** (1980) 38934.
11. H. Yan, J. Lu and E. Wang, *Chem. J. Chin. Univ.* (*English edition*) **4** (1988) 46.
12. H. Yan and J. Lu, *Sensors Actuators B.* **19** (1989) 33.
13. H. Yan and J. Lu, *Field Anal. Chem. Technol.* **1** (3) (1997) 175.
14. H. Yan and C.C. Liu, *Sensors Actuators B*, **17** (1994) 165.
15. Y. Wang, H. Yan and E. Wang, *J. Electroanal. Chem.* **497** (2001) 163.
16. Y. Wang, H. Yan and E. Wang, *Sensors Actuators B*, **87** (2002) 115.
17. S. Taguchi, A. Aramata and M. Enyo, *J. Electroanal. Chem.* **372** (1994) 161.
18. J. Giner, U.S.Patent No. 4729824 (1988).